Journal of Engineering Research

ISSN 2764-1317 vol. 5, n. 8, 2025

ARTICLE 6
Acceptance date: 24/11/2025

DYE-SENSITIZED SOLAR CELLS - DSSC: STRUCTURE-PROPERTY RELATIONSHIP OF CO-ADSORBENT

Luciano da Silva
Applied Chemistry Research Center, Department of Transformation Processes, Blvd Saltillo, Coah, Mexico

Karla Fabiola Rodriguez
Applied Chemistry Research Center, Department of Transformation Processes, Blvd Saltillo, Coah, Mexico

Harold Freeman
Polymer and Color Chemistry Program, North Carolina State University, Raleigh, NC, 27695, USA.

ABSTRACT: Two new compounds based on the phenyltetrazole system, 5-(4-octiloxyphenyl)tetrazole (LTz-3) and N,N-diethyl-4-{[(4'-nitro-2'-tetrazoyl)phenyl] diazenyl}aniline (SD-3), were synthesized and characterized as co-adsorbents in Dye--Sensitized Solar Cells (DSSCs). The effects of hydrophobic chain length and anchoring group on the properties of DSSCs containing the previously reported dye HD-14 and compared with the benchmark deoxycholic acid (DCA) are described. The charge-transfer resistance of dye/TiO_2 interface followed the order HD-14 – SD-3 > HD-14 – LTz-3 > HD-14 –DCA. However, the V_{OC} for the dye HD-14 with co-adsorbent DCA was 0.70 V, for the and the dye HD-14 with co-adsorbent LTz-3 was 0,70 V and for the dye HD-14 with co-adsorbent SD-3 was 0,67 V. Co-adsorbents LTz-3 and SD-3 achieved mean solar-to-power conversion efficiencies (%η), for three devices, of 9.22 and 7.50, respectively, compared to 8.90 for DCA under the same experimental device conditions. For LTz-3 co-adsorbent, the results can be attributed to the repellent effect of the long alkyl chain. For SD-3, it is possible that the volume of the co-adsorbent chain makes it difficult to form a more compact layer between the dye and the co--adsorbent. This allows the electrolyte to approaches, reducing the electron-injection efficiency into TiO2.

Keywords: Dye-Sensitized Solar Cells; Co--adsorbent; Tetrazole

Introduction

Dye-sensitized solar cells (DSSCs) based on nanocrystalline oxide semiconductors are a type of solar cells that convert the sun's energy to electric energy using a sensitizing dye [1-3]. A typical DSSC consists of a nanoparticle TiO_2 photoelectrode sensitized by a ruthenium bipyridine complex and a platinum counter-electrode separated by an iodide-triiodide (I^{-1}/I_3^{-1}) liquid electrolyte [4]. In DSSCs, the photosensitizer is a key component to harvest light and inject electrons. Until now, hundreds of photosensitizers have been designed and synthesized for improving the photovoltaic performance and exploring the relationship of structure and performance of DSSCs. Among them, the ruthenium complex dyes, such as N719, N3, C101 and HD14, have dominated the highly efficient DSSCs for many years [5- 8, 10]. For example, the efficiency of DSSC based on N719 has exceeded 12% [9]. However, the scarcity of ruthenium metal is a big problem for the future commercial development and applications. Compared with the metal complex dyes, the metal-free organic dyes have some advantages, such as the relative simplicity of synthesis and purification, convenient structural modification and high molar extinction coefficient. Thus, searching new metal-free organic dyes with excellent photovoltaic performance has attracted considerable attention. Many organic dyes, which exhibit comparably excellent photovoltaic performances to ruthenium complexes, have been designed and obtained [11-13]. However, designing the new organic dyes via simple and convenient synthetic routes is still a challenge in DSSCs. In last decade, various kinds of functional groups and their derivatives have been combined to generate D-p-A organic dyes. Among them, an arylamine group, thiophene derivatives and cyanoacrylic acid moiety are the most common subunits that act as an electron donor, p-linker, and an

electron acceptor/anchoring group, respectively. Especially, the p-linker as a bridge that connects the donor and acceptor exerts a significant influence on the transmission and recombination of electron during the photoelectric conversion process in DSSCs. Generally, the crucial step for the construction of D-p-A organic dyes is to connect the donor group and p-linker. The introduction of 1,2,3-triazole group as an electron deficient unit in the linear D-p-A organic dyes can effectively enhance the open-circuit voltage of the DSSCs with good efficiency [14]. The introduction of tetrazole group as an anchoring group has been related. The photovoltaic results further obtained with the tetrazole derivative outperformed those of the carboxylic analogue showing a significant increase in photovoltage for a device using the tetrazole dye [15].

Much effort has been paid to widen the light absorption by increasing the conjugation at both donor and p-linages. Unfortunately, their photovoltaic performance are still not significantly improved due to their aggregation during the photoelectrode fabrication process. Thus, co-sensitization using two or more sensitizers is an effective approach to achieve panchromatic harvest. Plenty work has been realized including ruthenium complex co-sensitized with an organic dye [16-25]. The co-sensitizations of organic dyes have been extensively investigated, which exhibit an effective and promising photovoltaic performance [26-31].

Here we report the photovoltaic performance of DSSCs derived from co-sensitization of HD14 and co-adsorbent SD3 and PTz-4 (**Fig. 1**).

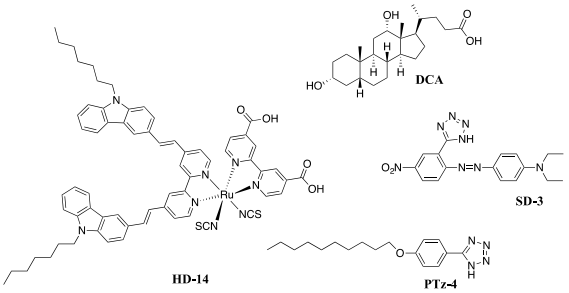

Fig. 1. Molecular structures of Dye (HD-14) and co-adsorbents: DCA, LTz-4 and SD-3.

Materials and Methods

General Information

The solvents and chemicals were purchased from Sigma-Aldrich, Fisher Scientific or TCI-America and used as received. The mass spectrometry analysis was carried out on a high-resolution mass spectrometer – Thermo Fisher Scientific Exactive Plus MS, a benchtop full-scan OrbitrapTM mass spectrometer using Heated Electrospray Ionization (HESI). Samples were dissolved in methanol and sonicated for 15 min. They were then diluted 1:1 with 20 mM ammonium acetate and analyzed via syringe injection into the mass spectrometer at a flow rate of 10 mL/min. The mass spectrometer was operated in negative ion mode. FT-IR (ATR) spectra were recorded on a Nicolet Nexus 470 FT-IR spectrometer (Thermo Scientific, USA) and UV-Visible spectra were measured by using Cary 300 spectrophotometer. Fluorescence, recorded at room temperature on a Fluorolog-3 spectrofluorometer (HORIBA Jobin Yvon Inc.). ^{1}HNMR (Hydrogen Nuclear Magnetic Resonance) and ^{13}CNMR (Carbon Nuclear Magnetic Resonance) spectra were recorded in a Bruker 500 MHz spectrometer.

Synthesis

Synthesis of 2-(1H-tetrazol-5-yl)-4-Nitro-benzenamine (1):

The synthesis of the tetrazole system (1) was carried out as depicted in the literature [32,33]. To a solution of 2-amino-5-nitrobenzonitrile (2) (7.0 g, 0.043 mol) in 28 mL N,N-dimethyl formamide (DMF) was added sodium azide (11.0 g, 0.17 mol) and ammonium chloride (9.0 g, 0.17 mol). The mixture was stirred for 24 h maintaining the temperature at 120 °C. The reaction mixture was cooled to room temperature and was poured into 50 mL of ice cold water. The mixture was acidified with concentrated HCl to pH 2. The precipitate formed was filtered off and the product was recrystallized from ethanol giving yellow crystals. Yield 65%; mp 264-266 °C; $mp_{Lit.}$ 268-270 °C [34]. FTIR-ATR ν_{max} = 3420, 2710–2630 (br), 1613, 1597, 1504, 1292, 842. ^{1}HNMR (500MHz, $CDCl_3$) δ = 7.45 (s, 1H, C_6H_3), 7.05 (d, J=8.4 Hz, 1H, C_6H_3), 6.62 (d, J=8.4 Hz, 1H, C_6H_3) 3.38 (br s, 1H, CN_4H). ^{13}CNMR (100 MHz, DMSO-d_6): 155.8 (1C), 137.3 (1C), 134.5 (1C), 117.1 (1C), 114.3 (1C), 112.6 (2C), 111.1(1C).

Synthesis of azo dyes N,N-diethyl-4-{[(4'-nitro-2'-tetrazoyl) phenyl]diazenyl} aniline (SD-3):

2-(1H-tetrazol-5-yl)-4-Nitro-benzenamine (2) (2.06 g, 0.01 mol) was dissolved in hydrochloric acid (20 mL) with stirring. After, the solution was cooled to 0 °C in an ice-bath. A solution of sodium nitrite (0.69 g, 0.01 mol) in 5mL water, cooled to 0 °C was added. The mixture was stirred for 30 min at 0 °C to get the clear diazonium salt solution. The coupling component N,N-diethylaniline (1.60 g, 0.01 mol) was dissolved in NaOH (15 mL, 1N) and then solution cooled 0 °C. To this well stirred solution, the above diazonium salt solution was added slowly so that temperature did not rise above 4 °C while maintaining the pH 4-5 by the action of sodium acetate solution (10% w/v). The mixture was stirred for 3 h at 0 °C. After, the solid obtained was collected by filtration, washed three times with cold water and dried. The crude product was recrystallized from hexane:ethylacetate (1:1). Violet crystals, 3,04 g, yield 83% m.p. >300 °C. FTIR-ATR: 1381.4 cm^{-1} and 1518.9 cm^{-1} (N-O stretch), 1603.1 cm^{-1} (C=C stretch). ^{1}H-NMR (500 MHz, DMSO-d_6): 8.69 (s, 1H), 8.45 (d, J = 10 Hz, 1H), 7.96 (d, J = 10 Hz, 1H), 7.76 (d, J=10 Hz, 2H), 6.87 (d, J=10 Hz, 2H), 3.50 (q, J = 5 Hz, 4H), 1.15 (t, J=5 Hz, 6H). ^{13}CNMR (100 MHz, DMSO-d_6): 153.4 (1C), 152.0 (1C), 146.2 (1C), 143.1 (1C), 127.5 (1C), 126.7 (1C), 125.8 (1C), 123.0 (1C), 117.2 (2C), 111.5 (2C), 44.4 (2C), 12.5 (2C). HRMS (ESI Full) m/z: calcd for $C_{17}H_{19}N_8O_2$ $[M+H]^+$, 367.1626; Found, 367.1636.

Synthesis of 5-(4-decyloxyphenyl)tetrazole (LTz-4):

To a round-bottomed flask were added 4-hydroxybenzonitrile (10.0 g, 0.084 mol), 1-bromodecano (18.6 g, 0.084 mol), KOH (46.4 g, 0.336 mol), and toluene/DMF (200 ml; 1:1) and the mixture was stirred under reflux for 6 h. The suspension was filtered and the solid was washed with toluene. The filtrate was concentrated and the obtained solid dissolved in diethylether. The organic

phase was washed with NaOH (5%; 50 ml), HCl (5%; 50 ml), and H_2O (50 ml) and dried over anhydrous Na_2SO_4. The product was obtained after removal of the solvent, as a white solid. To this solid (compound 2) were added NaN_3 (13.50 g; 0.208 mol), NH_4Cl (11.10 g, 0.208 mol) and DMF (100 ml) and the mixture was refluxed for 20 h. The suspension was cooled to room temperature and poured into 400 ml of ice/water and acidified to pH 3 using HCl, (10%). The mixture was filtered and the solid was washed several times with water. Recrystallization from ethanol gave a white solid; yield 65.0%, mp 164-166 °C, FT-IR ν_{max} = 3090, 2956, 2924, 2855, 3100–2600 (broad), 1627, 1522, 1345, 788. ^{1}H NMR (200 MHz, CDCl3) δ = 8.04 (d, J = 9.0 Hz, 2H, Ar-H), 7.14 (d, J = 9.0 Hz, 2H, Ar-H), 4.11 (t, J = 6.6 Hz, 2H, -CH_2O-), 1.81 (qui, J = 6.6 Hz, 2H, -C$\underline{H}_2$CH_2O-), 1.50 (m, 2H, -CH_2-), 1.24 – 1.40 (m, 12H, -CH_2-), 0.87 (t, J = 6.7 Hz, 3H, CH_3). ESI HRMS $[M+H]^+$ = Theo. M/z 247.15534; Found. M/z 247.15500, Error -1.366 ppm.

Synthesis of HD-14. HD-14 was synthesized according to the procedures reported by Cheema et al. [10].

Measurements of ground state oxidation potential (GSOP) by cyclic voltammetry

The experimental HOMO and E0-0 energy values for SD1, SD2, SD-3, SD-4, SD-5 and SD-6 were measured using a cyclic voltammetry (CV) whereas E0-0 was determined from the absorption onset of the relevant compound. The CV was carried in DMF with 0.1 M [TBA][PF_6] as an electrolyte at a scan rate of 50 mV s^{-1}. Glassy carbon was used as the working electrode (WE), Pt wire as counter electrode and Ag/Ag^+ in ACN was used as the reference electrode. Fc/Fc^+ was used as internal references, voltage measured was converted to NHE by addition of 0.63 V.

TiO2 electrode preparation and device fabrication

The photo-anodes composed of nanocrystalline TiO_2 and counter electrodes were prepared using a known procedure [35]. Fluorine-doped tin oxide (FTO) coated glasses (2.2 mm thickness, sheet resistance of 8 U/cm^2, TEC 8, Pilkington) were washed with detergent, water, acetone and ethanol, sequentially. After this FTO glass plates were immersed into a 40 mM aqueous TiCl4 solution at 70 °C for 30 min and washed with water and ethanol. Thin layer (8-12 mm thick) of TiO_2 (Solaronix, Ti-Nanoxide D/SP) was deposited (active area, 0.18 cm^2) on transparent conducting glass by squeegee printing. After drying the electrodes at 120 °C for 6 min, scattering layer (5 mm thick) TiO_2 particles (Solaronix, Ti- Nanoxide R/SP) were printed. The TiO_2 electrodes were heated under an airflow at 350 °C for 10 min, followed by heating at 500 °C for 30 min. After cooling to room temperature, the TiO_2 electrodes were treated with 40 mM aqueous solution of $TiCl_4$ at 70 °C for 30 min and then washed with water and ethanol. The electrodes were heated again at 500 °C for 30 min and left to cool to 80 °C before dipping into the dye solution. The dye solutions (0.3 mM) were prepared in 1:1:1 acetonitrile/t-butyl alcohol/DMSO. Deoxycholic acid was added to the dye solution as a coadsorbent at a concentration of 20 mM. The electrodes were immersed in the dye solutions with active area facing up

and then kept at 25 °C for 20 h to adsorb the dye onto the TiO_2 surface.

For preparing the counter electrode, pre-cut TCO glasses were washed with water followed by 0.1 M HCl in EtOH, and sonication in acetone bath for 10 min. These washed TCO were then dried at 400 °C for 15 min. Thin layer of Pt-paste (Solaronix, Platisol T/SP) on TCO was printed and the printed electrodes were then cured at 450 °C for 10 min. The dye sensitized TiO_2 electrodes were sandwiched with Pt counter electrodes and were sealed using a 40 µm Syrlyn spacer through heating of the polymer frame. The electrolyte (Solaronix, Iodolyte AN-50) was then injected into the cell, while the two electrodes were held together with the clips.

Photo-electrochemical measurements

Photocurrent-voltage characteristics of DSSCSs were measured using a Keithley 2400 source meter under illumination of AM 1.5 G solar light from solar simulator (SOL3A, Oriel) equipped with a 450 W xenon lamp (91160, Oriel). The incident light intensity was calibrated using a reference Si solar cell (Newport Oriel, 91150V) to set 1 Sun (100 mW cm^{-2}). The measurement was fully controlled by Oriel IV Test Station software. IPCE (incident monochromatic photon to current conversion efficiency) experiments were carried out using a system (QEX10, PV Measurements, USA) equipped with a 75 W short arc xenon lamp (UXL-75XE, USHIO, Japan) as a light source connected to a monochromator. Calibration of incident light was performed before measurements using a silicone photodiode (IF035, PV Measurements). All the measurements were carried out without the use of anti-reflecting film.

Electrochemical impedance spectroscopy (EIS)

The electrochemical impedance spectra were measured with an impedance analyzer potentiostat (Bio-Logic SP-150) under illumination using a solar simulator (SOL3A, Oriel) equipped with a 450 W xenon lamp (91160, Oriel). EIS spectra were recorded over a frequency range of 100 mHz - 200 kHz at room temperature. The applied bias voltage was set at the Voc of the DSSCSs, with AC amplitude set at 10 mV. The electrical impedance spectra were fitted using Z-Fit software (Bio-Logic).

Results and Discussion

Synthesis of co-adsorbents:

The synthesis of proposed co-adsorbent SD-3 and LTz-4 was carried out in the two-steps shown in **Scheme 1** and **Scheme 2**.

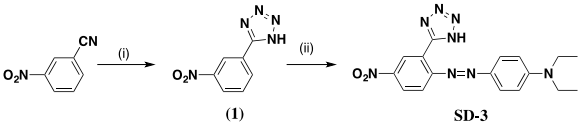

Scheme 1. Synthetic route of co-adsorbent SD-3. Reaction conditions: (i) = NaN_3/NH_4Cl/DMF, yield 65%; (ii) = $NaNO_2$, HCl, 5 °C, $C_6H_5N(-C_2H_5)_2$.

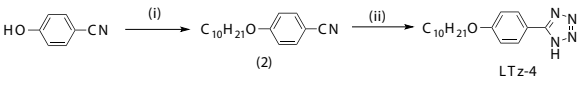

Scheme 2. Synthetic route of co-adsorbent LTz-4. Reaction conditions: (i) = $C_{10}H_{21}Br$, KOH, Toluene/DMF; (ii) = NaN_3/NH_4Cl/DMF, yield 65%.

In order to determine the practical utility of the synthesized molecules (LTz-4 and SD-3) as co-adsorbent in DSSCs, deoxycholic acid (DCA) was used as the standard and HD-14 was used as the dye. Nanocrystalline TiO_2 electrodes were prepared according to the procedure reported previously [35]. Sandwich types DSCs were prepared from the stained photodiodes and Pt coated cathode. Photovoltaic measurements were carried out after introducing the electrolyte between the glass electrodes.

Photophysical Measurements

The UV–Vis absorption and photoluminescence spectra of the co-adsorbent SD-3 and LTz-4 in DMF (concentration of 1,8 x 10^{-5} M) are depicted in Figure 2 and the corresponding photophysical data are summarized in **Table 1**.

Sensitizer	Experimental (eV)		
	[a]$E_{0\text{-}0}$ (eV)	[b,c]GSOP (E_{HOMO})	ESOP (E^*)
SD-3	1.98	-5.84	-3.83
LTz-4	4.28	-1.91	-6.19

[a] $E_{0\text{-}0}$ = calculated from the onset of absorption spectra (DMF).

[b] GSOP = ground state oxidation potential = E_{HOMO}.

[c] GSOP was measured in DMF with 0.1 M [TBA] [PF6] and with a scan rate of 50 mV s^{-1}. It was calibrated with Fc/Fc^+ as internal reference and converted to NHE by addition of 0.63 V; Excited-state oxidation potential ESOP (E*) was calculated from: E* = GSOP + E0-0

Table 1. Excited state oxidation potential – ESOP (E*), ground state oxidation potential (GSOP) and the lowest electronic transitions ($E_{0\text{-}0}$) for SD-3 and LTz-4.

In the electronic absorption spectra, the co-adsorbent SD-3 and LTz-4 exhibited a prominent band with the absorption maximum around 263 and 548 nm, respectively. The extinction coefficient are higher than 1.8 × 10^4 $M^{-1}cm^{-1}$. Such absorption characteristics can be ascribed to the π–π* transition of the whole D–π–A conjugation backbone. Similarly, the charge transfer emission maximum shifts from 610 nm for SD-3, 313 nm and 641 nm for LTz-4. These results suggest that LTz-4 dye possesses the strongest photoinduced intramolecular charge transfer ability over the π-conjugation backbone, leading to larger red shifts in absorption and emission spectra.

Photovoltaic parameters of DSCs

There are two widely used techniques for photovoltaic characterization: current–voltage measurements under simulated sunlight (producing J–V curves) and monochromatic light generated current measurements (producing incident photon-to-current conversion efficiency (IPCE) spectra). The photovoltaic parameters including short-circuit photocurrent density (J_{SC}), open- circuit voltage (V_{OC}), fill factor (FF) and overall power conversion efficiency (PCE) can be obtained by the current–voltage measurements. The IPCE value corresponds to the photocurrent density that is produced in the external circuit under monochromatic illumination of the cell divided by the photon flux that strikes the cell. The IPCE was determined by the light harvesting ability, the amount of adsorbed dyes on the TiO_2 surface, the overall charge collective efficiency and the overall electron injection efficiency. It is noted that the maximum IPCEs for DSCs generally should be smaller than 90% because of the reflection

and absorption loss due to the FTO glass. The **Fig. 2** shows the IPCE response as function of wavelength.

Incident photon to current conversion efficiency (IPCE) response of higher than 50% was exhibited by HD-14 – LTz-4 from 340 nm to 650 nm (reaching a maximum of 73% at 520-570 nm.) and by HD-14 – SD-3 from 390 nm to 560 nm (reaching a maximum of 55% at 410-420 nm). IPCE response high than 50% was achieved by HD-14 – DCA from 340 nm to 650 nm (reaching a maximum of 73% at 520-550 nm). These results indicate that, for this system, there is no direct relationship between amphiphilic characteristic and co-adsorbent effect for DSSCs. This possibility is confirmed by the result presented by the HD-14 - LTz-4 dye which one presented results very close to that presented by the HD-14 - DCA dye. On the other hand, the IPCE presented by the dye HD-14 – SD-3 was inferior to the result presented by the dye HD-14 – DCA, this must be probably due to the difficulty of anchoring on TiO_2 surface.

The photovoltaic parameters including the short-circuit photocurrent density (Jsc), open-circuit voltage (Voc), fill factors (ff) and overall cell efficiencies (%η) are summarized in Table 2 and I-V results are shown in **Fig. 3**. HD-14 – DCA resulted in photocurrent densities (Jsc) of 19.50 mA cm^{-2}, HD-2 – LTz-4 resulted in Jsc of 19.71 mA cm^{-2} and HD-2 – SD-3 resulted in Jsc of 17.22 mA cm^{-2}, respectively. The fact that some compositions have higher values of photocurrent density can be attributed to the co-adsorbent favoring of photons capture and the more favorable injection of electrons into TiO_2. The dye HD-14 – DCA resulted in open-circuit photovoltage (V_{OC}) of 0.71 V, the dye HD-14 – LTz-4, resulted in V_{OC} of 0.70 V and the dye HD-14 – SD-3, resulted in V_{OC} of 0.67 V.

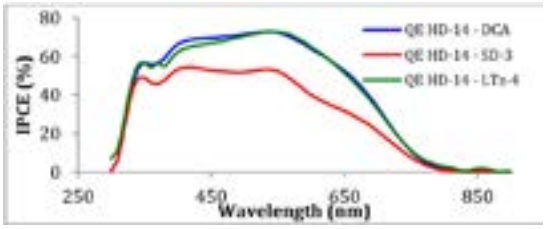

Fig. 2. Photocurrent action spectra (IPCE) obtained with the dyes HD-14 – DCA, HD-14 – LTz-4, and HD-14 – SD-3. The concentration of the co-adsorbent used was 20 mM for all dyes.

DYE[a]	Voc [b] (V)	Jsc [b] (mA/ cm2)	Fill Factor[b]	Efficiency[b] (%)	Best Efficiency (%)
HD-14 – DCA	0,71	19.50 ± 0.04	0,67	9.14 ± 0.09	9.22
HD14 – LTz-4	0,70	19.71 ± 0.01	0,67	9.20 ± 0,01	9.21
HD-14 – SD-3	0,67	17.22 ± 0.02	0,65	7.48 ± 0,01	7.49

[a] Concentration of 0.3 mM in 1:1:1 acetonitrile/t-butyl alcohol/DMSO. The concentration of the co--adsorbent was 20 mM for all dyes.

[b] Averages taken over 3 to 4 devices.

Table 2. Photocurrent–voltage characteristics of DSSCs sensitized with HD-14 – DCA, HD14 – LTz-4 and HD-14 – SD-3.

The use of LTz-4 as a co-adsorbent was shown to be more efficient. The dye HD-14 - LTz-4 resulted in a Jsc of 19.71 mA cm^{-2} and Voc of 0.70 V, translating into a total conversion efficiency (%η) of 9.21% and, the dye HD-14 – SD-3 resulted in a Jsc of 17.22 mA cm^{-2} and Voc of 0.67 V, translating into a total conversion efficiency (%η) of 7.48%, while the benchmark HD-14 - DCA show a total conversion efficiency (%η) of 9.22%.

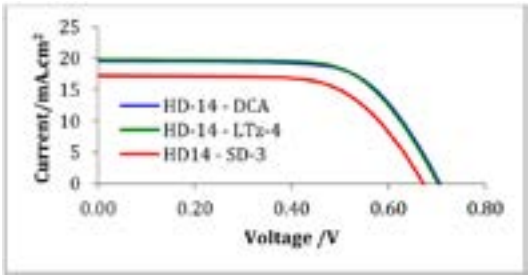

Fig. 3. Photocurrent–voltage characteristics of DSCs sensitized with HD-14 – DCA, HD-14 – LTz-4 and HD-14 – SD-3. The concentration of the co-adsorbent used was 20 mM for all dyes.

Electrochemical impedance spectroscopy

Electrochemical impedance spectroscopy (EIS) successfully models the charge transfer and chemical capacitance at the interface of TiO_2 dye/electrolyte and Pt/electrolyte in DSSC under operational conditions. Combination of charge transfer resistance (Rct) and chemical capacitance gives rise to a semi circle at the complex plan. Combination of charge transfer resistance and chemical capacitance give rise to a semi circle at the complex plan. In a typical EIS experiment, the first semicircle at high frequency corresponds to the cathode in a DSC, the middle semicircle corresponds to charge transfer resistance at the interface of dye/TiO_2 combined with chemical capacitance of electrons in TiO_2 ($eTiO_2$), and the third semicircle corresponds to finite Warburg impedance element [37-38]. The studies indicate that to the middle semicircle, the increase in its diameter is due to retardation of the charge recombination resistance (Rrec) at the interface of the TiO2/dye/electrolyte.

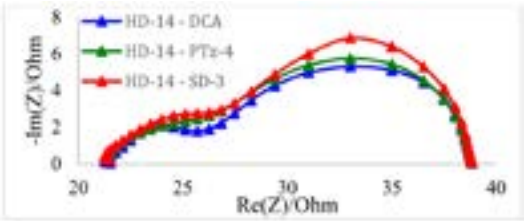

Fig. 4. EIS Nyquist plots for DSSCs sensitized with HD-14 – DCA, HD-14 – LTz-4 and HD-14 – SD-3.

In Nyquist plot (Fig. 4), the middle frequency semicircles were in the following order of increased charge recombination resistance HD-14 – SD-3 > HD-14 – LTz-4 > HD-14 – DCA, which was in the order of the actual photovoltage obtained from the corresponding solar devices. Thus, the higher the charge recombination resistance in Nyquist plot, the higher the photovoltage obtained from solar cells will be owing to slower charge recombination of electrons in TiO_2 ($eTiO_2$) and electron acceptors in electrolyte, resulting in higher $eTiO_2$ lifetime [39-42].

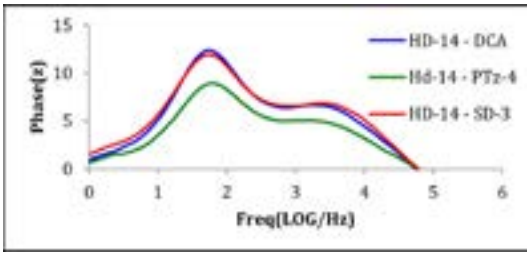

Fig. 5. EIS Bode plots for DSCs sensitized with HD-14 – DCA, HD-14 – LTz-4 and HD-14 – SD-3.

In Fig. 5, the frequency response in the range of 1-100 Hz indicates the recombination of $eTiO_2$ with electrolyte as the function of $eTiO_2$ lifetime. The injected electron lifetime $eTiO_2$ can be determined by using the relation ($\tau CB = 1/(2\pi f)$, where τ is the lifetime of electrons in TiO_2 and f is the mid-frequency peak in Bode plots. $eTiO_2$ depends on the density of charge traps, which is ultimately related to V_{oc}. In other words, the Bode plot results complement the Nyquist plot. The frequency peak of the DSCs in the range of 1-100 Hz based on HD-14, with different co-adsorbents were at 53Hz, corresponding to $eTiO_2$ of 3.0ms, respectively, thus resulting in similar V_{oc} for different co-adsorbent, which correlates well with the actual V_{oc} reported for the solar cells (Table 2). A similar trend was also observed in the Nyquist plots (Figure 4).

The tetrazole system allows identification of two distinct effects that correlate with the magnification of the photovoltaic effect. The first one is related to the amphiphilic characteristic of the co-adsorbent and the second effect is related to the capacity of formation of the compact layer between co-adsorbent and dye.

Considering the amphiphilic character of co-adsorbent LTz-4, which has a 10-carbon alkyl chain, we believe that its greater contribution is due to the more protected monolayer formation capacity [43]. The hydrophobic end acts as a buffer between the semiconductor and the electrolyte, thus effectively preventing back-transfer of electrons from the semiconductor's CB to the redox couple or the oxidized dye molecules, so that unwanted re-combination is reduced [44-46]. On the other hand, the co-adsorbents SD-3 does not have an amphiphilic characteristic, which reduces its photoconversion efficiency, compared to that of the co-adsorbent DCA.

Long alkyl chain can suppress the dye aggregation on the TiO_2 film during dye uptake process and improve the device efficiency. Such an improvement is mainly observed in the organic dyes [47]. In case of Ru-based (octahedral) small size dyes, like HD-14, dye aggregation is not so strong and a compact monolayer on the TiO_2 film can form easily, resulting in a long electron lifetime [48]. One possible reason for the high efficiency HD-14 – LTZ-4 based DSC can be attributed to the bulkiness of the co-adsorbent dye set, leading to more compact monolayer formation, which hinders the recombination of conduction band electrons back to the electrolyte. Considering that the overall performance of DSSCs depends on the electron injection efficiency, we suggest that the improved IPCE performance of DSSCs based on the LTz-4 may arise from the prevention of the deactivation of the excited state via quenching processes between dye and co-adsorbent. The planarity of the bi-isonicotinic acid system and the near-planar phenyltetrazole system (the tetrazole and phenyl rings have a dihedral angle of 14.8 (1)° between the planes) [49], the strong hydrogen bonds and π-π interactions can occur. The results of this strongly interactions are the formation of a more compact layer that allows charge-transfer from dye to the phenyltetrazole system by π-π stacking interactions that improve electron-injection efficiency into TiO_2. Massin and co-workers observed that the tetrazole anchoring group is very similar to a carboxylate group. The strong interaction between TiO_2 and the carboxylate group was evidenced by two short Ti–O distances (2.09 Å), which correspond to a bridge coordination mode. In

the case of tetrazole as the anchoring group, the optimized geometry indicated that the interaction of the tetrazole with the surface occurs through a short Ti – N distance (2.53 Å) and an additional longer one (3.48 Å) [50]. Thus, similarly to the carboxylic acid derivative, the tetrazole-end-capped adopts a strong chemisorption-like coordination mode to attach to TiO_2. With this in mind, it can be stated that the anchoring group tetrazole, can exert the same effect as the carboxylic acid anchoring group, allowing an alternative approach to enhancing the efficiency of electron injection into TiO_2.

Conclusion

The development of new materials for DSSCs and understanding the interaction between them remains a major challenge in creating innovative hybrid materials with valuable functionality. In the present study, new phenyltetrazole derivatives were evaluated as co-adsorbents with HD-14 dye attached to TiO_2 thin films. The photovoltaic performance of phenyltetrazoles in DSSCs, were explored and compared to DCA co-adsorbent. Overall, the results demonstrate the effectiveness of the tetrazole functional group as an alternative co-adsorbent moiety for organic photosensitizers. Structural characteristics of the evaluated co-adsorbents allow the distinction of two effects that contribute to enhancing the efficiency of photo-injection in DSSCs. Theses effects allows more efficient charge transfer from dye to the phenyltetrazole system by π-π stacking interactions, that improves electron-injection efficiency into TiO_2. These results demonstrate a strong dependence of the electron injection process on TiO_2 to increase the efficiency of DSSCs.

Acknowledgements

The author, Karla Fabiola Rodríguez Ramírez, thanks CONACYT for granting her a scholarship to carry out her doctoral studies at CIQA. The authors gratefully acknowledge the financial support of SECIHTI CBF2023-2024-3604. Authors wish to thank National Laboratory of Graphene (CONACYT-232753) for the facilities support. The authors wish to thank Dr. Hammad Cheema for providing the sample of HD-14 used in this investigation.

References

[1] O'Regan B, Gra¨tzel M. A low-cost, high-efficiency solar cell based on dye-sensitized colloidal TiO_2films. Nature 1991;353:737-740.

[2] Kalyanasundaram K, Ed., Dye-sensitized solar cells, EPFL press, Lausanne, 2010.

[3] Hagfeldt A, Boschloo G, Sun L, Kloo L, Pettersson H. Dye-Sensitized Solar Cells. Chem Rev 2010;110:6595-6663.

[4] Magne C, Dufour F, Labat F, Lancel G, Durupthy O, Cassaignon S, Pauporte T. Effects of TiO_2 nanoparticle polymorphism on dye-sensitized solar cell photovoltaic properties. J Photochem Photobiol A 2012; 232:22-31.

[5] Nazeeruddin M K, Pechy P, Renouard T, Zakeeruddin SM, Humphry-Baker R, Comte P, et al. Engineering of efficient panchromatic sensitizers for nanocrystalline TiO2-based

solar cells. J Am Chem Soc 2001;123:1613-1624.

[6] Gao F, Wang Y, Shi D, Zhang J, Wang M, Jing X, et al. Enhance the optical absorptivity of nanocrystalline TiO2 film with high molar extinction coeffi- cient ruthenium sensitizers for high performance dye-sensitized solar cells. J Am Chem Soc 2008;130:10720-10728.

[7] Chen C, Wang M, Li J, Pootrakulchote N, Alibabaei L, Ngoc-le CH, et al. Highly efficient light-harvesting ruthenium sensitizer for thin-film dye-sensitized solar cells. ACS Nano 2009;3:3103-3109.

[8] Chou C, Wu K, Chi Y, Hu W, Yu S, Lee G, et al. Ruthenium(II) sensitizers with heteroleptic tridentate chelates for dye-sensitized solar cells. Angew Chem Int Ed 2011;50:2054-2058.

[9] Ito S, Nazeeruddin MK, Liska P, Comte P, Charvet R, Pechy P, et al. Photovoltaic characterization of dye-sensitized solar cells: effect of device masking on conversion efficiency. Prog Photovolt 2006;14:589-601.

[10] Cheema H, Islam A, Younts R, Gautam B, Bedja I, Gupta R K, El-Shafei A. More stable and more efficient alternatives of Z-907: carbazole-based amphiphilic Ru(ii) sensitizers for dye-sensitized solar cells. Phys Chem Chem Phys 2014;16(48):27078–27087.

[11] Zhang G, Bala H, Cheng Y, Shi D, Lv X, Yu Q, et al. High efficiency and stable dye-sensitized solar cells with an organic chromophore featuring a binary pconjugated spacer. Chem Commun 2009; 2198-200.

[12] Im H B, Kim S K, Park C M, Jang S H, Kim C J, Kim K K, et al. High performance organic photosensitizers for dye-sensitized solar cells. Chem Commun 2010;46:1335-1337.

[13] Zeng W, Cao Y, Bai Y, Wang Y, Shi Y, Zhang M, et al. Efficient dye-sensitized solar cells with an organic photosensitizer featuring orderly conjugated ethylenedioxythiophene and dithienosilole blocks. Chem Mater 2010;22: 1915-1925.

[14] Heredia D, Natera J, Gervaldo M, Otero L, Fungo F, Lin CY, et al. Spirobi- fluorene-bridged donor/acceptor dye for organic dye-sensitized solar cells. Org Lett 2010;12:12-15.

[15] Massin J, Ducasse L, Toupance T, Olivier C. Tetrazole as a New Anchoring Group for the Functionalization of TiO2 Nanoparticles: A Joint Experimental and Theoretical Study, J Phys Chem C 2014;118:10677–10685.

[16] Ogura R Y, Nakane S, Morooka M, Orihashi M, Suzuki Y, Noda K. High-performance dye-sensitized solar cell with a multiple dye system. Appl Phys Lett 2009;94:073308,1-3.

[17] Holliman P J, Davies M L, Connell A, Velasco B V, Watson T M. Ultra-fast dye sensitisation and co-sensitisation for dyesensitized solar cells. Chem Commun 2010;46:7256-7258.

[18] Fan S Q, Kim C, Fang B, Liao K X, Yang G J, Li C J, Kim J J, Ko J. Improved Efficiency of over 10% in Dye-Sensitized Solar Cells with a Ruthenium Complex and an Organic Dye Heterogeneously Positioning on a Single TiO_2 Electrode. J Phys Chem C 2011;115:7747-7754.

[19] Han L, Islam A, Chen H, Malapaka C, Chiranjeevi B, Zhang S, Yang X, Yanagida M. High-efficiency dye-sensitized solar cell with a novel co-adsorbent. Energy Environ Sci 2012; 5:6057-6060.

[20] Nguyen L H, Mulmudi H K, Sabba D, Kulkarni S A, Batabyal S K, Nonomura K, Grätzel M, Mhaisalkar S G. A selective co-sensitization approach to increase photon-

conversion efficiency and electron lifetime in dye-sensitized solar cells. Phys Chem Chem Phys 2012;14:16182-16186.

[21] Ozawa H, Shimizu R, Arakawa H. Significant improvement in the conversion efficiency of black-dye-based dye-sensitized solar cells by cosensitization with organic dye. RSC Adv 2012;2:3198-3200.

[22] Zhang S, Islam A, Yang X, Qin C, Zhang K, Numata Y, Chen H, Han L. Improvement of spectral response by co-sensitizers for high efficiency dye-sensitized solar cells. J Mater Chem A 2013;1:4812-4819.

[23] Singh S P, Chandrasekharam M, Gupta K S V, Islam A, Han L, Sharma G D. Efficiency of ruthenium dye sensitized solar cells enhanced by 2,6-bis[1-(phenylimino)ethyl] pyridine as a co-sensitizer containing methyl substituents on its phenyl rings. Org Electron 2013;14:1237-1241.

[24] Lee C L, Lee W H, Yang C H. The effects of co-sensitization in dye-sensitized solar cells. J Mater Sci 2013;48: 3448-3453.

[25] Qin C, Numata Y, Zhang S, Islam A, Yang X, Sodeyama K, Tateyama Y, Han L. A Near-Infrared cis-Configured Squaraine Co-Sensitizer for High-Efficiency Dye-Sensitized Solar Cells. Adv Funct Mater 2013, 23, 3782-3789.

[26] Chen Y, Zeng Z, Li C, Wang W, Wang X, Zhang B. Highly efficient co-sensitization of nanocrystalline TiO_2electrodes with plural organic dyes. New J Chem 2005;29:773-776.

[27] Kuang D, Walter P, Nüesch F, Kim S, Ko J, Comte P, Zakeeruddin S M, Nazeeruddin M K, Grätzel M. Co-sensitization of Organic Dyes for Efficient Ionic Liquid Electrolyte-Based Dye-Sensitized Solar Cells. Langmuir 2007;23:10906-10909.

[28] Yum J H, Jang S R, Walter P, Geiger T, Nüesch F, Kim S, Ko J, Grätzel M, Nazeeruddin M K. Efficient co-sensitization of nanocrystalline TiO_2 films by organic sensitizers. Chem Commun 2007;4680-4682.

[29] Magne C, Urien M, Pauporté T. Enhancement of photovoltaic performances in dye-sensitized solar cells by co-sensitization with metal-free organic dyes. RSC Adv 2013, 3, 6315-6318.

[30] Pang A, Xia L, Luo H, Li Y, Wei M. Highly efficient indoline dyes co-sensitized solar cells composed of titania nanorods. Electrochim Acta 2013, 94, 92-97.

[31] Zhang M, Wang Y L, Xu M F, Ma W T, Li R Z, Wang P. Design of high-efficiency organic dyes for titania solar cells based on the chromophoric core of cyclopentadithiophene-benzothiadiazole. Energy Environ Sci 2013;6:2944-2949.

[32] Silva L, Gallardo H, Magnago R, Begnini I M. Liquid Crystals Containing the Isoxazole and Tetrazole Heterocycles. Mol Cryst Liq Cryst 2005;432:1-13.

[33] Santos D R, Oliveira A G S, Coelho R L, Begnini I M, Magnago R F, Da Silva L. Synthesis of liquid crystals materials derived from oxadiazole, isoxazole and tetrazole heterocycles. ARKIVOC 2008;v.XVII:157-166.

[34] Akhlaghinia B, Rezazadeh S. A Novel Approach for the Synthesis of 5-Substituted-1H-tetrazoles. J Braz Chem Soc 2012;23(12):2197-2203.

[35] Ito S, Murakami T N, Comte P, Liska P, Grätzel C , Nazeeruddin M K ,etal. Fabrication of thin film dye sensitized solar cells with solar to electric power conversion efficiency over 10%. Thin Solid Films 2008;516:4613-4619.

[36] Nazeeruddin M K, Splivallo R, Liska P, Comte P, Grätzel M. A swift dye uptake

procedure for dye sensitized solar cells. Chem Commun 2003;1456-1457.

[37] Wang Q,. Moser J E, Gräatzel M. Electrochemical impedance spectroscopic analysis of dye-sensitized solar cells, J Phys Chem B 2005;109:14945-14953.

[38] Bisquert J, Theory of the impedance of charge transfer via surface states in dye-sensitized solar cells, J Electroanal Chem 2010;646:43-51.

[39] Kalyanasundaram K, Dye-Sensitized Solar Cells, CRC ; Taylor & Francis, Boca Raton, Fla.; London, 2009.

[40] Fabregat-Santiago F, Bisquert J, Garcia-Belmonte G, Boschloo G, Hagfeldt A. Influence of electrolyte in transport and recombination in dye-sensitized solar cells studied by impedance spectroscopy. Sol Energy Mater Sol Cells 2005;87:117-131.

[41] Gaes M S, Joanni E,. Muniz E C, Savu R, Habeck T R, Bueno P R, Fabregat- Santiago F. Impedance Spectroscopy Analysis of the Effect of TiO_2 Blocking Layers on the Efficiency of Dye Sensitized Solar Cells. J Phys Chem C 2012;116:12415-12421.

[42] Wu K, Ku W, Clifford J N, Palomares E, Ho S, Chi Y, Liu S, Chou P, Nazeeruddin M K, Grätzel M. Harnessing the open-circuit voltage *via* a new series of Ru(II) sensitizers bearing (*iso*-)quinolinyl pyrazolate ancillaries. Energy Environ Sci 2013;6:859-870.

[43] Yen Y S, Lin T Y, Hsu C Y, Chen Y C, Chou H H, Tsai C, Lin J T. A remarkable enhancement of efficiency by co-adsorption with CDCA on the bithiazole-based dye-sensitized solar cells, Org Electron 2013;14:2546-2554.

[44] Zhang Z, Evans N,. Zakeeruddin S M, Humphry-Baker R, Grätzel M. Effects of ω-Guanidinoalkyl Acids as Coadsorbents in Dye-Sensitized Solar Cells. J Phys Chem C 2007;111:398-403.

[45] Wang M, Li X, Lin H, Pechy P, Zakeeruddin S M, Grätzel M, Passivation of nanocrystalline TiO2 junctions by surface adsorbed phosphinate amphiphiles enhances the photovoltaic performance of dye sensitized solar cells. Dalton Trans 2009;10015-10020.

[46] Wang Z S, Cui Y, Dan-oh Y, Kasada C, Shinpo A, Hara K. Thiophene-Functionalized Coumarin Dye for Efficient Dye-Sensitized Solar Cells: Electron Lifetime Improved by Coadsorption of Deoxycholic Acid. J Phys Chem C 2007;111:7224-7230.

[47] Mayor L C, Taylor J B, Magnano G, Rienzo A, Satterley C J, O'Shea J N, Schnadt J. Photoemission, resonant photoemission, and x-ray absorption of a Ru(II) complex adsorbed on rutile Ti O 2 (110) prepared by in situ electrospray deposition. J Chem Phys 2008;129:114701-9.

[48] Bonomo M, Saccone D, Magistris C, Di Carlo A, Barolo C, Dini D. Effect of Alkyl Chain Length on the Sensitizing Action of Substituted Non-Symmetric Squaraines for p-Type Dye-Sensitized Solar Cells. Chem Electro Chem 2017;4(9):2385–2397.

[49] Gallardo H, Begnini I M, Vencato I, 5-(4-Hydroxyphenyl)tetrazole--Water (2/3); Acta Cryst 1997;C53:143-144.

[50] Massin J, Ducasse L, Toupance T, Olivier C. Tetrazole as a New Anchoring Group for the Functionalization of TiO2 Nanoparticles: A Joint Experimental and Theoretical Study. J Phys Chem C 2014;*118(*20):10677-10685.